Spatial pooling of contrast in contrast gain control

Michael D'Zmura and Benjamin Singer*

Department of Cognitive Sciences and Institute for Mathematical Behavioral Sciences, University of California, Irvine, Irvine, California 92697

Received November 30, 1995; revised manuscript received June 7, 1996; accepted July 1, 1996

We report psychophysical measurements of spatial pooling functions for contrast gain control. We use a nulling technique to measure the dependence of contrast induction on the spatial frequency of a sinusoidal contrast modulation. This dependence on spatial frequency, when transformed, provides the profile of a spatial pooling function. The measured profiles are fitted well by Gaussians. We confirm earlier results that the area over which spatial pooling takes places depends on the scale of the modulated pattern. We also find that pooling functions are similar for achromatic and isoluminant stimuli. © 1996 Optical Society of America.

Key words: contrast, gain control, spatial frequency.

1. INTRODUCTION

Models of contrast gain control measure the local contrast in the response of a bank of linear spatial filters by integrating the rectified or squared responses of the filters across an appropriate spatial pooling area.[1–5] This spatially pooled measure of contrast is then used to set local contrast gain.

Cannon and Fullenkamp[6] used a central disk and an annular surround to provide the first estimates of spatial pooling areas. They varied the area of the surround, which comprised a spatially sinusoidal modulation at 2, 4, or 8 cycles per degree (c/deg) of visual angle. A contrast-matching technique was used to measure the apparent contrast of the central disk, formed of a sinusoid with a frequency identical to that of the surround. They found that the apparent contrast functions at these spatial frequencies overlay one another when plotted as a function of surround width in cycles. Cannon and Fullenkamp's result is that the linear extent of spatial pooling is proportional to the wavelength of the sinusoidal stimulus.

We also estimated spatial pooling areas.[4] Following Chubb *et al.*,[7] we modulated in time the contrast of an annular surround and used a nulling technique to measure the apparent modulation of contrast in a central disk. We tried two methods to estimate spatial pooling areas and found similar results, using both achromatic and isoluminant stimuli, the latter along the long- and middle wavelength-sensitive- (L&M-) cone and along the short-wavelength-sensitive- (S-) cone axes.[8–11] With the first method we varied the size of the annular area in which contrast is modulated. Results showed that increasing the area of the annulus produces an increase in the apparent modulation of disk contrast that levels off exponentially for annulus outer radii between 2 and 3 deg of visual angle. With the second method, we varied the distance from the central disk of a ring in which contrast was modulated. The area of the ring was held constant. Results showed that increasing the ring distance produces a decrease in the apparent modulation of disk contrast that levels off exponentially for ring inner radii between 2 and 3 deg of visual angle. We used binary spatial noise for disk and annulus in these experiments; the peak in its spatial-frequency spectrum was at ~1.8 c/deg. The effective widths of 4–6 deg of visual angle that we found agree roughly with those found by Cannon and Fullenkamp when they used sinusoids at 2 c/deg.

Although these two sets of data help to specify spatial pooling functions for contrast gain control, they give little indication of how contrast is pooled within the central area subtended by the disk. How can one measure complete pooling functions—ones without a central hole?

In this paper we introduce a new way to measure the spatial pooling area for contrast gain control. We modulate the contrast modulation of an annular region by using a spatial sinusoid and vary the spatial frequency of the sinusoidal contrast modulation to determine the dependence of apparent contrast induction on spatial frequency. Transforming spatial-frequency sensitivity into the space domain provides the profile of a complete pooling function. This work was described elsewhere in preliminary form.[12]

2. METHODS

Observers viewed a disk and an annulus made of binary spatial noise (see Fig. 1). The stimulus was centered on a gray background. Stimulus contrast was modulated sinusoidally in time at 1 Hz. Stimulus contrast was also modulated by a spatial sinusoid, so that the total contrast modulation was a spatially sinusoidal counterphase flicker. Observers used a nulling technique to measure the strength of contrast induction within the disk area.

The detailed methods are similar to those described in previous papers.[4,5] Disk and annulus were displayed on a Sony Trinitron GDM-1961 color monitor that was viewed at a distance of one m. Software on a DECstation 3000/400 computer controlled a Turbo PXG+ graphics board, which generated a 1280 × 1024 pixel display at 66 Hz noninterlaced. We measured the spectra, chromaticities, and luminances of the monitor's three phosphors, using a Photo Research PR-650 SpectraColorimeter, and appropriate entries in the color lookup tables were used to correct for the nonlinearity between applied voltage and

0740-3232/96/1102135-06$10.00

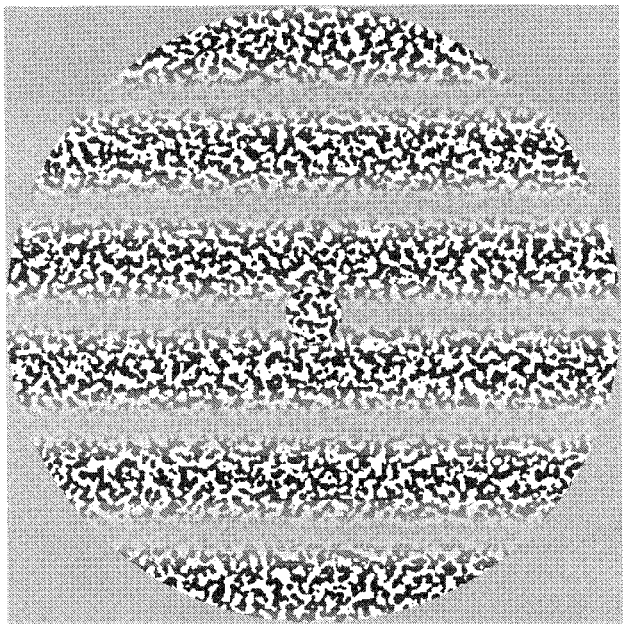

Fig. 1. Stimulus spatial properties. A binary noise carrier is used to form a central disk and an annular surround of diameter 16 deg of visual angle. The annular surround is modulated sinusoidally both in space and in time. Although this is also true of the central disk, in this figure the central disk contrast modulation is chosen to provide an appearance of uniform contrast. A medium-grain stimulus is pictured.

phosphor intensity. The screen displayed a steady, gray background of luminance 52 cd/m^2 and CIE 1931 standard observer (x, y) chromaticity (0.28, 0.30).

The diameter of the stimulus was 16 deg of visual angle (see Fig. 1). The disk diameter was 1 deg of visual angle, which corresponded to 64 pixels. Disk and annulus comprised binary noise of variable grain size. We computed the noise carrier by first creating a spatially isotropic difference-of-Gaussians amplitude spectrum. The second step was to use a random-phase spectrum to construct, through an inverse Fourier transform, noise in the space domain. Finally, the noise was binarized to make spatially isotropic binary noise that, for the largest grain size, had a peak in its spatial-frequency power spectrum at ~1.45 c/deg. Noise carriers at two smaller sizes were generated by dividing the spatial standard deviations in the difference-of-Gaussians amplitude spectrum by either 2 or 4. The peak spatial frequencies were thus approximately 1.45, 2.9, and 5.8 c/deg for coarse-, medium-, and fine-grain carriers, respectively.

We modulated stimulus chromatic properties by using color animation. Chromatic properties are described in a color space based on Krauskopf's cardinal axes.[9–11] As described in a previous paper,[5] these axes include the achromatic axis, the L&M-cone axis, and the S-cone axis; the last two were determined by calculation with the Smith–Pokorny[8] fundamentals.

The contrast of the disk and annulus was modulated by a static, spatial sinusoid of variable spatial frequency. This space-modulated contrast was then modulated sinusoidally in time at 1 Hz, so producing a counterphase-flickering grating of contrast modulation.

The annulus stimulus is described by a space- and time-varying color vector $\mathbf{A}(\mathbf{x}, t)$. This three-dimensional vector in color space is a linear combination of the vector $\mathbf{w}$ that represents the gray background and the annulus mean contrast vector $\mathbf{a}_m$, which is modulated in space and time:

$$\mathbf{A}(\mathbf{x}, t) = \mathbf{w} + b_A(\mathbf{x})\{\mathbf{a}_m[1 + \alpha \cos(2\pi f y)\sin(2\pi t)]\}, \quad (1)$$

in which $b_A(\mathbf{x})$ describes the dependence of the annulus binary noise pattern on position $\mathbf{x} = (x, y)$ and takes values ± 1 within the annulus area and 0 elsewhere, α represents the amplitude of the contrast modulation, and f is the spatial frequency in cycles per degree of the spatial modulation of contrast. The vertical displacement y has units of degrees of visual angle; the center of the stimulus is taken as the origin for the determination of spatial phase. The central disk is described as a similar combination of the neutral background $\mathbf{w}$ and the disk mean contrast $\mathbf{d}_m$:

$$\mathbf{D}(\mathbf{x}, t) = \mathbf{w} + b_D(\mathbf{x})\{\mathbf{d}_m[1 + \delta \cos(2\pi f y)\sin(2\pi t)]\}, \quad (2)$$

in which $b_D(\mathbf{x})$ describes the spatial dependence of the disk binary noise carrier pattern and δ is the amplitude of the disk contrast modulation.

We used the method of limits to help determine nulling contrast modulations, as detailed in an earlier paper.[4] The observers' task was to find the amplitude of nulling modulation that was required to eliminate the apparent change in disk appearance caused by modulating the contrast of the annulus. The physical nulling modulation so found is a measure of the strength of the induced modulation of apparent contrast. Each experimental run had two ascending and two descending sequences, each with 11 trials, presented in alternation. For each run, the average of the four upper and the four lower thresholds provides the estimate of the nulling contrast modulation that is reported below.

The authors, BS and MD, participated as observers in the experiments. Each has normal color vision as tested with Ishihara plates[13] and was properly refracted.

3. RESULTS

We measured the dependence of spatial pooling areas on the scale of the stimulus carrier pattern and on the color properties of the stimulus.

A. Dependence on Carrier Scale

We set the mean contrast of the disk and the annulus to 0.25; the maximum modulation of annulus contrast was fixed at the same value. Annulus contrast thus varied between 0.0 and 0.50. We chose these modest contrast levels to avoid saturating nonlinearities in the response of the contrast gain control to contrast modulation.[4,5] The resulting contrast induction was measured across a range of spatial frequencies for coarse-, medium-, and fine-scale carriers.

The dependence of nulling contrast modulation on the spatial frequency of the inducing modulation and on the scale of the carrier pattern is shown in Fig. 2. Results in

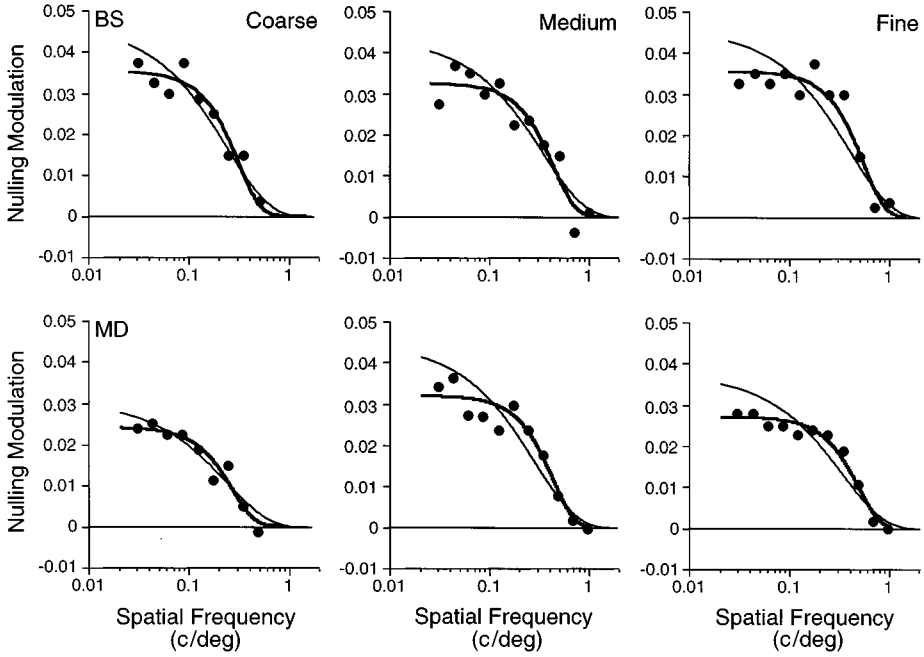

Fig. 2. Dependence of nulling contrast modulation on the spatial frequency of the contrast modulation and on the scale of the carrier pattern. Panels in the left, middle, and right columns describe results for coarse- (1.45 c/deg), medium- (2.9 c/deg), and fine-grain (5.8 c/deg) achromatic stimuli, respectively. Panels in the top and bottom rows describe results for observers BS and MD, respectively. The spatial frequency of the contrast modulation varies along the horizontal axis of each plot, and the amplitude of the disk contrast modulation that is needed to null the induced modulation varies along the vertical axis. The 11 spatial frequencies for data points in the top middle panel are as follows, from left to right: 0.031, 0.044, 0.063, 0.088, 0.125, 0.177, 0.25, 0.35, 0.5, 0.71, and 1.0 c/deg. The heavy curves show the best-fit Gaussian functions. The light curves show the best-fit exponential functions.

Table 1. Parameters of Gaussian and Exponential Fits to the Data in Fig. 2[a]

	Scale		
Subject parameter	Coarse	Medium	Fine
BS			
Gaussian	(0.035, 0.233)	(0.032, 0.325)	(0.035, 0.415)
	91.4	90.7	92.4
Exponential	(0.047, 4.389)	(0.044, 3.194)	(0.046, 2.770)
	89.3	84.4	75.3
MD			
Gaussian	(0.024, 0.202)	(0.032, 0.321)	(0.027, 0.375)
	91.8	93.7	97.8
Exponential	(0.031, 4.506)	(0.048, 3.767)	(0.038, 3.277)
	89.3	83.6	82.1

[a] For each panel in Fig. 2, Gaussian parameters (a, σ) of Eq. (3) are listed above the exponential parameters (b, β) of Eq. (4). Shown immediately below each pair of parameters is the percentage of variance accounted for (R^2) by the fit.

the left, middle, and right columns were found for coarse-, medium-, and fine-grain carriers, respectively. Results in the top and bottom rows were obtained by observers BS and MD, respectively. The spatial frequency of the contrast modulation varies along the horizontal axis of each panel; the nulling modulation amplitude is marked along the vertical axis.

The heavy curves in Fig. 2 show the best-fit[14] Gaussians to the data points; these have the form

$$y = a \exp[-0.5 * (x/\sigma)^2]. \quad (3)$$

We also fitted exponentials, which captured the data nearly as well (light curves, Fig. 2). The exponentials have the form

$$y = b \exp(-\beta x). \quad (4)$$

The parameters (a, σ) of the Gaussian fits and (b, β) of the exponential fits to the data in the six panels of Fig. 2 are listed in Table 1; also listed are the percentages of variance accounted for by each of the fits.

In Fig. 3 we plot the standard deviations of the space-domain Gaussians that best fit the data. The space-domain Gaussians are found through an inverse Fourier transform of the spatial-frequency-domain Gaussians; their standard deviations are related reciprocally.[15] The standard deviations are plotted as a function of the peak spatial wavelength of the noise carrier pattern.

The standard deviations increase monotonically with carrier wavelength. Both observers' data are fitted well by lines. For BS, the best-fit line relating standard deviation y and carrier peak wavelength x has equation $y = 3.62x + 1.8$, and for MD the best-fit line has equation $y = 4.54x + 1.75$. We can thus estimate crudely the linear extent of spatial pooling, taken as ± 1, namely, two standard deviations, to be approximately eight times carrier wavelength, plus 1.8 deg of visual angle. The linear increase in the extent of contrast pooling with carrier peak wavelength agrees with the earlier result of Cannon and Fullenkamp.[6] The two sets of results differ in that the linear increase found here is not a proportional increase as they suggested; the intercepts of the best-fit lines to the data in Fig. 2 differ from zero.

B. Stimulus Color Properties

The dependence of nulling contrast modulation on the chromatic properties of the stimulus is shown in Fig. 4 for observers BS (top row) and MD (bottom row). In these experiments, we chose stimulus lights to lie along the L&M-cone axis (middle column) or the S cone axis (right column). The mean contrast was set to 0.25 of the maximum displayable contrast along each axis. The maximum displayable contrast to the L cones along the L&M-cone axis is 0.082, and the maximum displayable contrast to the S cones along the S-cone axis is 0.89. The maximum modulation of annulus contrast was fixed at 0.25 of the maximum displayable contrast, so that annulus contrast varied between 0.0 and 0.5 of the maximum displayable contrast, or between 0.0 and 0.041 to L cones along the L&M-cone axis and between 0.0 and 0.445 to S cones along the S-cone axis.

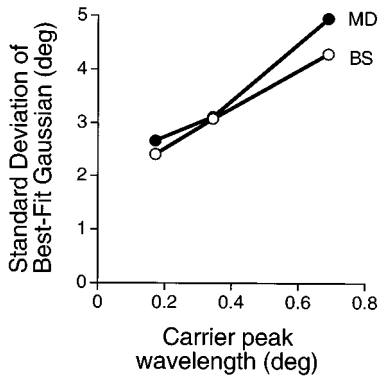

Fig. 3. Standard deviations of the space-domain Gaussians that describe contrast pooling at three carrier scales for two observers. The best-fit Gaussians in Fig. 2 are transformed into the space domain to provide the Gaussians whose standard deviations are shown here at carrier peak spatial frequencies of 1.45, 2.9, and 5.8 c/deg, which correspond to wavelengths of 0.69, 0.34, and 0.17 deg of visual angle, respectively.

We used medium-grain stimuli in these experiments. We compare the results with the colored stimuli to those found earlier with medium-scale achromatic stimuli; the data in the Achromatic panels of Fig. 4 (left column) are identical to those in the corresponding panels in Fig. 2 (BS, Medium and MD, Medium). Results for the isoluminant stimuli are plotted in terms of contrast to L cones for stimuli along the L&M-cone axis and in terms of contrast to S cones for S-cone-axis stimuli.

The results found with the isoluminant stimuli are fitted well by Gaussians, which are shown as heavy curves in Fig. 4. The exponential fits, shown as light curves, are nearly as good. The parameters of the Gaussian and the exponential fits are listed in Table 2, as are the percentages of variance accounted for by the fits.

Figure 5 shows the standard deviations of the best-fit Gaussians in the space domain for observers BS (filled bars) and MD (open bars). While there is a tendency for the standard deviations to be slightly larger for the S-cone stimuli than for the achromatic stimuli, we have no reason at the moment to believe that these differences are significant. Rather, the results suggest clearly that there is no difference in spatial pooling for achromatic and isoluminant stimuli.

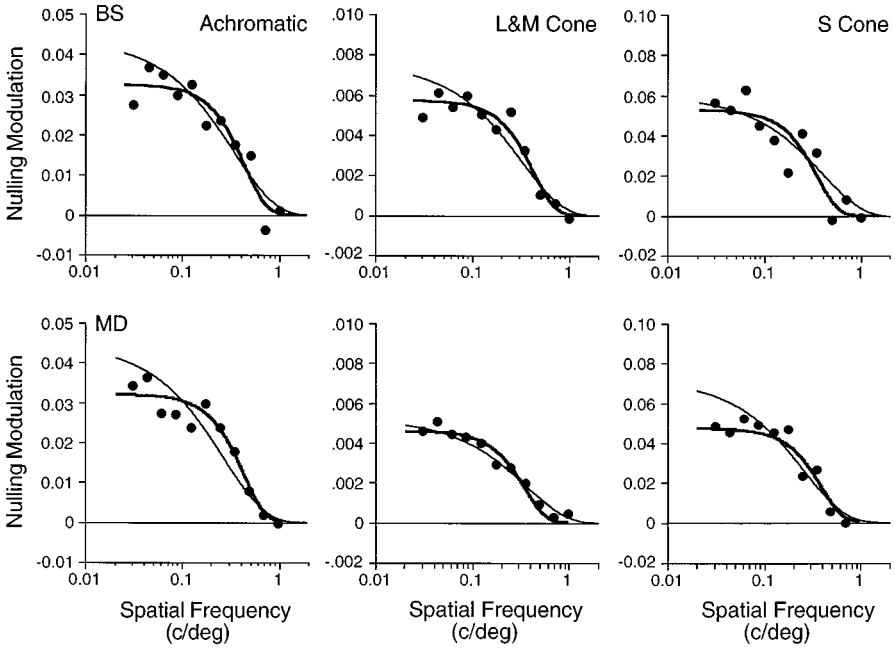

Fig. 4. Dependence of nulling contrast modulation on contrast modulation spatial frequency for medium-grain stimuli presented along the achromatic axis (left column), the L&M-cone axis (middle column), and the S-cone axis (right column) for observers BS (top row) and MD (bottom row). The results for achromatic stimuli duplicate the corresponding ones in Fig. 2, middle column. The units of the vertical scale for the plots in the middle column are in terms of L-cone contrast. The units of the vertical scale for the plots in the right column are in terms of contrast to S-cones. The heavy curves show the best-fit Gaussian functions, and the light curves show the best-fit exponential functions.

Table 2. Parameters of Gaussian and Exponential Fits to the Data in Fig. 4[a]

	Stimulus		
Subject	Achromatic	L&M Cone	S Cone
BS			
Gaussian	(0.032, 0.325)	(0.0057, 0.315)	(0.053, 0.265)
	90.6	95.5	83.1
Exponential	(0.044, 3.194)	(0.0076, 3.408)	(0.061, 2.653)
	83.3	83.8	81.9
MD			
Gaussian	(0.032, 0.321)	(0.0046, 0.262)	(0.046, 0.285)
	93.2	96.5	93.7
Exponential	(0.048, 3.767)	(0.0053, 2.989)	(0.071, 4.331)
	83.9	96.6	79.2

[a] For each panel in Fig. 4, Gaussian parameters (a, σ) of Eq. (3) are listed above the exponential parameters (b, β) of Eq. (4). Estimates of amplitude parameters a and b are in units of achromatic contrast, contrast to L cones, and contrast to S cones for achromatic, L&M-cone-, and S-cone-axis stimuli, respectively. Shown immediately below each pair of parameters is the percentage of variance accounted for (R^2) by the fit.

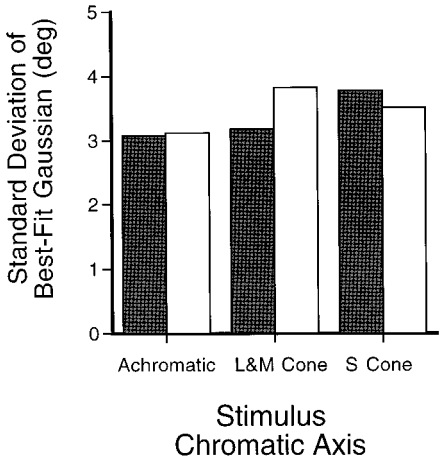

Fig. 5. Standard deviations of the space-domain Gaussians that describe contrast pooling for achromatic and isoluminant stimuli for two observers. The best-fit Gaussians in Fig. 4 are transformed to the space domain to provide the Gaussians whose standard deviations are shown here for observers BS (filled bars) and MD (open bars) for achromatic, L&M-cone, and S-cone stimuli.

4. DISCUSSION

The results show that spatial-frequency sensitivities for the spatial pooling of contrast are low-pass functions that are fitted well by Gaussians. The sensitivities are fitted well also by exponential functions and, presumably, by a number of other functions. We prefer the Gaussian model for its simplicity and wide applicability in the modeling of visual processing.[16]

With the Gaussian model we estimate the linear extent of spatial pooling, taken as ± 1 standard deviation, to be roughly eight times carrier wavelength plus 1.8 deg of visual angle. This rule provides estimates that are a bit larger than the earlier ones.[4,6] For instance, our earlier estimate of a linear extent of 4–6 deg for a carrier peak frequency of 1.8 c/deg is somewhat smaller than the estimate $6.24 = 8 \times (1/1.8) + 1.8$ provided by the present rule. However, there is every reason to believe that the present estimates are more accurate. One problem that hinders a direct comparison of these results with those of Cannon and Fullenkamp[6] is the compound spectrum of the binary noise. Although the binary noise has a narrow peak in its energy spectrum at its peak frequency, it possesses energy at all other frequencies, too, so that no one spatial frequency is perfectly isolated, as would be more nearly the case with a sinusoidal carrier.

The present results suggest that differences in spatial pooling of contrast for stimuli along achromatic, L&M-cone, and S-cone axes are small. This agrees with the results of our earlier work.[4] We recall here the argument against differences in spatial pooling, namely that differences could cause contrast modulations in one location to cause space-varying change in the chromatic contrast properties of neighboring areas. For instance, a small space constant for isoluminant contrast and a large one for achromatic contrast could lead a contrast increase with components along both achromatic and isoluminant axes to cause a significant reduction in apparent achromatic contrast, but not isoluminant contrast, at a far enough distance from the modulation. The results of the earlier work[4] and of the present experiments suggest that this source of differential induction is negligible.

A fundamental limitation of the present results is the unexamined assumption of linearity. The inverse Fourier transform of the frequency-domain results into the space domain is informative only if the spatial pooling of contrast is linear. Although we used stimuli of small and moderate contrast in an attempt to avoid saturating and other nonlinearities, we did not test whether the spatial pooling of contrast was linear. One can examine this question experimentally by making separate measurements of contrast induction for spatial modulations at two different spatial frequencies and then seeing whether the sum of the two spatial modulations produces the sum of the inductions, for many pairs of spatial frequencies. Zaidi and his colleagues[17,18] have conducted experiments that begin to get at this important question.

Several other interesting experiments that extend the present results remain to be done. First, one naturally would like to know whether spatial pooling areas are spatially isotropic. For instance, it may be that contrast pooling areas for oriented carrier patterns are elongated along the major axis of the carrier. We can assess this property by using an oriented carrier of fixed orientation (e.g., horizontal) and measuring spatial-frequency sensitivities at two or more contrast modulation orientations (e.g., horizontal and vertical). Second, the spatial pooling functions presented here depend on our choice of 1° for central disk diameter. Preliminary measurements reported by us[12] on the dependence of contrast induction on central disk diameter suggest clearly that induction increases as disk size decreases. A more systematic study of this dependence is needed. Third, the applicability of the present approach would be greater if sinusoidal carriers rather than binary noise carriers are used. We used binary noise because of display limitations. One particular problem with the noise carrier is the presence of lumi-

nance artifacts associated with the display of the nominally isoluminant stimuli along the L&M-cone and the S-cone axes. We discussed this issue thoroughly in two earlier papers.[4,5] Such artifacts can be minimized by the use of horizontally oriented sinusoidal carriers of modest spatial frequency.

We described a bilinear model for chromatic selectivity in contrast gain control in earlier work.[5] The basic assumption that underlies the model is that the change in color contrast at a point, as a result of the action of contrast gain control, is related linearly both to the color signal at that point and to the color contrast in the surrounding area. To test the model, we performed psychophysical experiments that examined the effects of modulating the contrast of an annulus on the apparent contrast of a central disk. The results of the experiments let us specify the chromatic components of the model numerically so that precise predictions concerning chromatic selectivity in contrast gain control could be made. Using the knowledge of the spatial pooling of contrast provided by the present experiments, we can extend the model to predict the effects of contrast gain control on the visual processing of color images.[19]

ACKNOWLEDGMENTS

We thank Geoffrey Iverson, Kenneth Knoblauch, Christopher Tyler, and Qasim Zaidi for their helpful suggestions. This work was supported by National Eye Institute grant EY10014 to M. D'Zmura.

*Present address, Center for Visual Science, Meliora Hall, University of Rochester, Rochester, New York 14627

REFERENCES

1. G. Sperling, "Three stages and two systems of visual processing," Spatial Vision **4**, 183–207 (1989).
2. D. J. Heeger, "Normalization of cell responses in cat striate cortex," Visual Neurosci. **9**, 181–197 (1992).
3. J. A. Solomon, G. Sperling, and C. Chubb, "The lateral inhibition of perceived contrast is indifferent to on-center/off-center segregation, but specific to orientation," Vis. Res. **33**, 2671–2683 (1993).
4. B. Singer and M. D'Zmura, "Color contrast induction," Vis. Res. **34**, 3111–3126 (1994).
5. B. Singer and M. D'Zmura, "Contrast gain control: a bilinear model for chromatic selectivity," J. Opt. Soc. Am. A **12**, 667–685 (1995).
6. M. W. Cannon and S. C. Fullenkamp, "Spatial interactions in apparent contrast: inhibitory effects among grating patterns of different spatial frequencies, spatial positions and orientations," Vis. Res. **31**, 1985–1998 (1991).
7. C. Chubb, G. Sperling, and J. A. Solomon, "Texture interactions determine perceived contrast," Proc. Natl. Acad. Sci. (USA) **86**, 9631–9635 (1989).
8. V. C. Smith and J. Pokorny, "Spectral sensitivity of the foveal cone photopigments between 400 and 500 nm," Vision Res. **15**, 161–171 (1975).
9. D. I. A. MacLeod and R. M. Boynton, "Chromaticity diagram showing cone excitation by stimuli of equal luminance," J. Opt. Soc. Am. **69**, 1183–1186 (1979).
10. J. Krauskopf, D. R. Williams, and D. M. Heeley, "The cardinal directions of color space," Vision Res. **22**, 1123–1131 (1982).
11. A. M. Derrington, J. Krauskopf, and P. Lennie, "Chromatic mechanisms in lateral geniculate nucleus of macaque," J. Physiol. (London) **357**, 241–265 (1984).
12. M. D'Zmura, B. Singer, L. Dinh, J. Kim, and J. Lewis, "Spatial sensitivity of contrast induction mechanisms," presented at the 1994 OSA Annual Meeting, Dallas, Tex., October 2–7, 1994.
13. S. Ishihara, *The Series of Plates Designed as a Test for Colour-Blindness* (Kanehara, Tokyo, 1986).
14. K. R. Gegenfurtner, "PRAXIS: Brent's algorithm for function minimization," Behav. Res. Meth. Instrum. Comput. **24**, 560–564 (1993).
15. R. N. Bracewell, *The Fourier Transform and its Applications*, 2nd ed. (McGraw-Hill, New York, 1978).
16. J. Robson, "Spatial and temporal contrast-sensitivity functions of the visual system," J. Opt. Soc. Am. **56**, 1141–1142 (1966).
17. Q. Zaidi, B. Yoshimi, N. Flanigan, and A. Canova, "Lateral interactions within color mechanisms in simultaneous induced contrast," Vis. Res. **32**, 1695–1707 (1992).
18. J. S. DeBonet and Q. Zaidi, "Weighted spatial interaction of induced contrast-contrast," Invest. Ophthalmol. Vis. Sci. **35** (Suppl.), 1667 (1994).
19. M. D'Zmura, B. Singer, and C. Li, "A bilinear model for contrast gain control," Invest. Ophthalmol. Vis. Sci. **36** (Suppl.), S392 (1995).